

Research paper

Physicochemical properties of amorphous precipitates of cimetidine–indomethacin binary system

Shigeo Yamamura*, Hiroaki Gotoh, Yoko Sakamoto, Yasunori Momose

School of Pharmaceutical Sciences, Toho University, Miyama 2-2-1, Funabashi, Chiba, Japan

Received 6 October 1999; accepted in revised form 6 December 1999

Abstract

We have found that the binary system, consisting of a precipitate of cimetidine and naproxen, became amorphous due to intermolecular interaction. In order to clarify the interaction between cimetidine and other drugs, the physicochemical properties of binary systems consisting of cimetidine and drugs, phenacetin, salicylamide or indomethacin, were investigated. X-ray powder diffraction patterns and thermal analysis findings for the precipitates indicated that the cimetidine–indomethacin system has an amorphous structure, whereas the cimetidine–phenacetin and cimetidine–salicylamide systems do not. Fourier-transform infra-red (FTIR) spectroscopy and nuclear magnetic resonance (NMR) spectroscopy findings suggested that there is an intermolecular interaction between a proton in the imidazole ring of cimetidine and the C=O in the COOH of indomethacin. Since an interaction by the hydrogen bond between cimetidine and indomethacin would prevent three-dimensional arrangements of the molecules, the precipitate would be amorphous. In the cimetidine–indomethacin system, decarboxylation of indomethacin occurred below the melting temperature, indicating that the chemical stability decreased upon precipitation. Cimetidine was found to interact with drugs with a carboxyl group. The interaction would be applicable to make the amorphous system of the drugs and increase the solubility of the drugs. © 2000 Elsevier Science B.V. All rights reserved.

Keywords: Intermolecular interaction; Amorphous; Chemical shift; Cimetidine; Indomethacin

1. Introduction

It is well known that the bioavailability of drugs with poor water solubility is influenced by their dissolution characteristics [1–3]. Numerous methods to modify the dissolution characteristics have been investigated to improve their bioavailability [4–9]. The degree of crystallinity is one of the important factors governing the dissolution rate, and consequently, the bioavailability of drugs [10]. In the case of drugs with poor water solubility, amorphous preparations are sometimes used in the field of pharmaceutical sciences to improve the bioavailability [11–14]. Several methods of preparing amorphous solids have been investigated including lyophilization [15], spray-drying [16], cogrinding [11] and super-cooling the melt [14]. There have been several reports on the preparation of amorphous solids using polymers [17–19]. Many authors have discussed the view that an interaction between the drugs and the polymer used is responsible for the formation of the amorphous solid.

Small molecules have been used as excipients to form an amorphous (glassy) system can be achieved by cooling the melts [20–21].

In a previous study, we found that an amorphous precipitate was obtained only upon evaporation of an ethanol solution of the cimetidine–naproxen system without heating, and that a molecular interaction occurs between cimetidine and naproxen in the solid state and in solution [22]. There are few reports of the amorphous system being made due to the molecular interaction between small molecular drugs without heating.

In the present study, we prepared precipitates of the binary system of cimetidine and some drugs with various molecular characteristics (indomethacin, salicylamide and phenacetin) from ethanol solutions, and solid state characteristics of the precipitates were studied by X-ray powder diffraction, thermal analysis and Fourier-transform infra-red (FTIR) spectroscopy. In the cimetidine–indomethacin system, the precipitates were found to become amorphous, and the interaction between two drugs in solution and in solid state was investigated by some spectroscopic methods. Pharmaceutical properties, such as physicochemical stability and the phase solubility diagram of the cimetidine–indomethacin system, were also investigated.

* Corresponding author. School of Pharmaceutical Sciences, Toho University, Funabashi, Chiba 274-8510, Japan. Tel.: +81-47-472-1350; fax: +81-47-472-1350.

E-mail address: yamamura@phar.toho-u.ac.jp (S. Yamamura)

2. Materials and methods

2.1. Materials

Cimetidine (CIM; Tokyo Kasei Co., Tokyo, Japan), phenacetin (PHEN; Sigma Chemical Co., St. Louis, MO), salicylamide (SA; Tokyo Kasei Co.) and indomethacin (INDO; Sigma Chemical Co.) were used as received. All other reagents were of reagent grade. The molecular structure of each of the drugs used in the present study is shown in Fig. 1.

2.2. Methods

2.2.1. Preparation of precipitates of CIM-drug binary system

CIM (1 g) and the drug in various molar ratios was dissolved in 100 ml of ethanol, and then the solvent was evaporated under reduced pressure at 40°C. Hereafter, the ratio of CIM and the other drug are given as mol.%, i.e. (20:80) represents a composition of 20 mol.% of CIM and 80 mol.% of the other drug. The residual solvent in the precipitate was removed completely by placing the sample under a vacuum for at least 2 days in a desiccator containing P₂O₅. The precipitates were stored in a desiccator with silica gel until use in the experiments.

2.2.2. X-ray diffractometry (powder method)

X-ray powder diffraction patterns were obtained using a RINT 2500 X-ray diffractometer (Rigaku Co., Tokyo, Japan). The X-ray source was Cu K α radiation at a voltage of 50 kV and a current of 100 mA. The diffracted X-ray beam was monochromated by means of a bent-type graphite monochromator, and a scintillation counter was used as the detector. Diffraction intensities were measured by a fixed-time step-scanning method in the range of 5–40° (2 θ) at an interval of 0.02°.

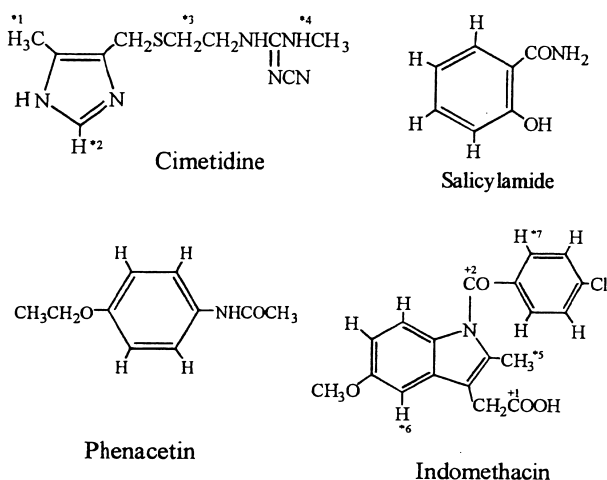


Fig. 1. Molecular structure of cimetidine, phenacetin, salicylamide and indomethacin. The meaning of *1–*7 and +1 to +2 is given in section 3.2.

2.2.3. Thermal analysis

Differential scanning calorimeter (DSC) curves were obtained with a DSC 3100S (MAC Science Co., Kanagawa, Japan) under N₂ gas flow (100 ml/min). Thermogravimetric analysis-differential thermal analysis (TG-DTA) curves were obtained with a TG-DTA 2010S (MAC Science Co.). A quadrupole mass spectrometer equipped with a TG-DTA system was also used (TG-DTA/MS, model VG, MAC Science Co.) to investigate the cause of weight loss during heating. Sample powders were packed in an aluminium sample pan (open type) and heated at a rate of 10°C/min. The weight of the sample powder was about 10 mg for DSC measurements and 20 mg for TG-DTA and TG-DTA/MS measurements.

2.2.4. High-performance liquid chromatography (HPLC)

HPLC chromatograms were recorded using a PU-980 + UV-980 system (Nihon Bunko Co., Tokyo, Japan) to check the degradation. An octadecyl silica (ODS) column was used and the mobile phase consisted of methanol–acetonitrile–water (75:10:5). The flow rate was 0.5 ml/min, and ultraviolet absorption was monitored at 215 nm.

2.2.5. FTIR

FTIR spectra were obtained by means of an FTIR spectrophotometer (FTIR-500, Nihon Bunko Co.) equipped with a diffuse reflectance attachment (DR-81, Nihon Bunko Co.). The measurements were attempted with the accumulation of 1000 scans and a resolution of 4 cm⁻¹ over the range of 600–4000 cm⁻¹.

2.2.6. Nuclear magnetic resonance (¹H-NMR and ¹³C-NMR)

¹H-NMR and ¹³C-NMR spectra were recorded using a JEOL Alpha 500 spectrometer (Nihon Denshi Co., Tokyo, Japan) at 50°C to decrease the viscosity of the solvent. About 40 mg of sample was dissolved in 0.8 ml of DMSO-*d*₆. Chemical shifts are expressed in δ (ppm) downfield from the internal standard (tetramethylsilane).

2.2.7. Phase solubility determinations

The phase solubility diagrams for CIM and drug systems in ethanol were determined at 37°C. An excess amount of the drug was added to 5 ml of ethanol containing various amounts of CIM in test tubes with a stopper. The test tubes were kept in a constant-temperature bath maintained at 37°C for at least 66 h. Then the solution was appropriately diluted with ethanol, and the concentration of the drug was determined by an ultraviolet (UV) absorption method using a spectrophotometer (U-3300 Hitachi Co., Tokyo, Japan). The concentration in solution was determined in triplicates.

3. Results

3.1. Characterization of CIM-NSAIDs precipitates

Figs. 2 and 3 show X-ray powder diffraction patterns and TG-DTA curves for the precipitates of the CIM-PHEN, CIM-SA and CIM-INDO systems, respectively (the content of CIM is 50 mol.% in each instance). The diffraction patterns of the CIM-PHEN and CIM-SA systems showed sharp diffraction peaks of crystalline drugs, and endothermic peaks attributable to melting were observed in DTA curves. No changes in the positions of diffraction peaks were observed upon precipitation, indicating that modification of the crystalline properties did not occur upon precipitation of the CIM-PHEN and CIM-SA binary systems, whereas diffraction peaks disappeared in the diffraction pattern of the precipitate of the CIM-INDO system. Furthermore, an endothermic peak, attributable to melting, was not observed in the DTA curve of the CIM-INDO system (the small endothermic peak in the vicinity of 70°C will be discussed later). These results indicate that the CIM-INDO system became amorphous only upon precipitation. No additional peaks were detected in HPLC chromatograms of any of the precipitates, indicating that no degradation occurred upon precipitation.

Figs. 4 and 5 show the changes in the X-ray powder diffraction pattern and the TG-DTA curves, respectively for CIM-INDO systems prepared with various compositions. Amorphous precipitates of CIM-INDO were obtained

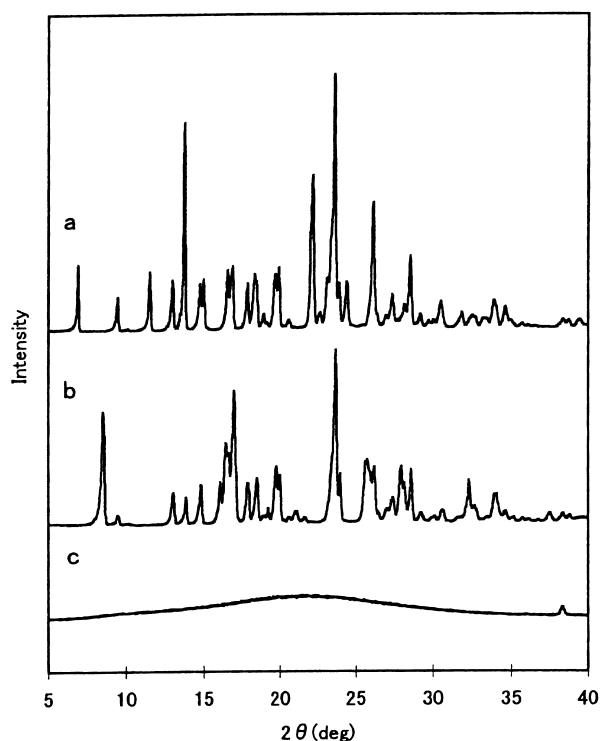


Fig. 2. X-ray diffraction patterns of precipitates of binary systems: (a), CIM-PHEN (50:50); (b), CIM-SA (50:50); (c), CIM-INDO (50:50).

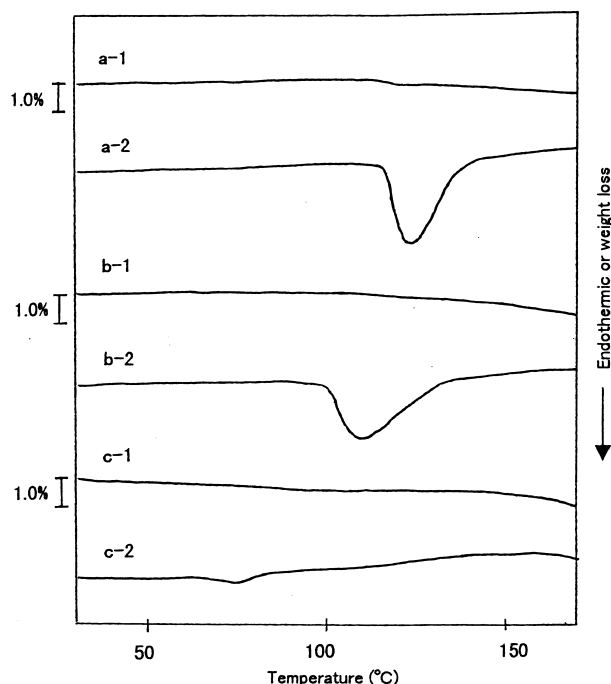


Fig. 3. TG-DTA curves for precipitates of binary systems. (a-1, a-2) TG and DTA curves for CIM-PHEN (50:50); (b-1, b-2), TG and DTA curves for CIM-SA (50:50); (c-1, c-2), TG and DTA curves for CIM-INDO (50:50).

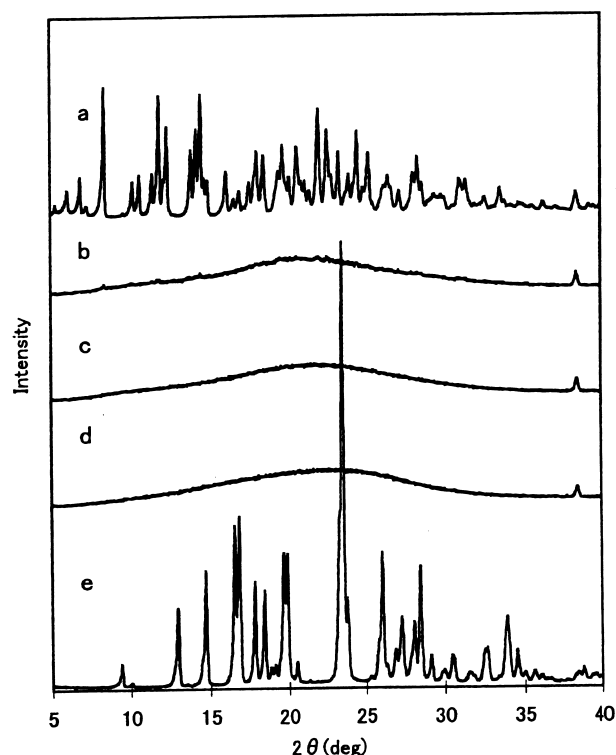


Fig. 4. X-ray diffraction patterns of CIM-INDO precipitates prepared with various compositions: (a), CIM-INDO (0:100); (b), CIM-INDO (20:80); (c), CIM-INDO (50:50); (d), CIM-INDO (80:20); and (e), CIM-INDO (100:0).

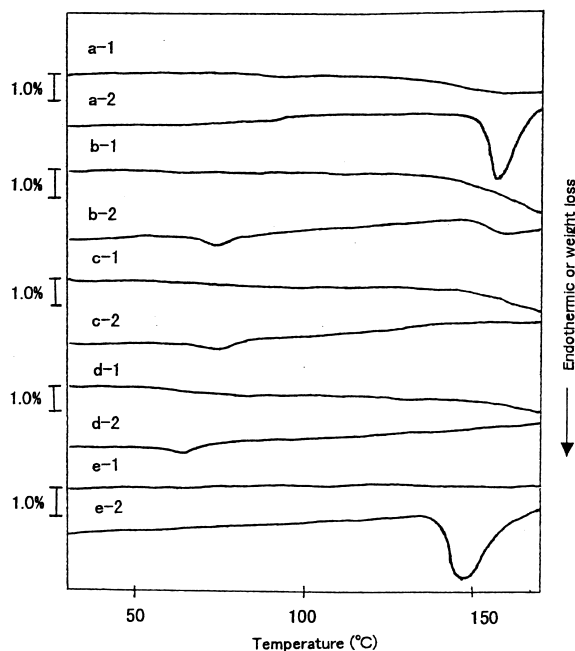


Fig. 5. TG-DTA curves for CIM-INDO precipitates prepared with various compositions. (a-1, a-2) TG and DTA curves for CIM-INDO (0:100); (b-1, b-2), TG and DTA curves for CIM-INDO (20:80); (c-1, c-2), TG and DTA curves for CIM-INDO (50:50); (d-1, d-2), TG and DTA curves for CIM-INDO (80:20); (e-1, e-2), TG and DTA curves for CIM-INDO (100:0).

in systems with a CIM content in the range of 20–80%. As indicated by the X-ray powder diffraction pattern, α -INDO was found to crystallize by precipitation of INDO solely.

Fig. 6 shows the FTIR spectra of CIM-INDO systems with various compositions. The FTIR spectra of the CIM-INDO systems became broad upon precipitation. The peak at 1735 cm^{-1} , attributable to $\nu_{\text{C=O}}$ in the carboxyl group of α -INDO [23], became weak and was associated with broad neighboring peaks. In the FTIR spectra of the CIM-PHEN and CIM-SA systems, there were few changes upon precipitation.

3.2. NMR chemical shift of CIM and INDO in solution

Interaction between CIM and INDO molecules was investigated by NMR spectroscopy. The chemical shifts of protons and carbons were measured by ^1H -NMR and ^{13}C -NMR spectroscopy. Figs. 7 and 8 show the change in chemical shift of some protons and carbons, respectively of CIM and INDO depending on the CIM content. In ^1H -NMR analysis of the CIM-INDO system, a chemical shift of a proton in the imidazole ring of CIM (*2 in Fig. 1, observed at 7.45 ppm) of about 0.06 ppm to a lower magnetic field was observed with increasing INDO content. A small change in the chemical shift of H in $-\text{NHCH}_3$ of CIM (*4 in Fig. 1, observed at 7.24 ppm) was also observed. In the CIM-PHEN and CIM-SA systems, no significant changes in ^1H -NMR chemical shift were observed with change in composition of these systems.

With respect to the ^{13}C -NMR chemical shifts, there were no significant changes in any of the carbons in the CIM-PHEN, CIM-SA or CIM-INDO systems, except for C in the COOH of INDO (+1 in Fig. 1, 171.89 ppm). Fig. 8 shows the chemical shifts of two carbons (+1 and +2 in Fig. 1) in INDO with increasing CIM content. Although a chemical shift of C in the COOH (+1 in Fig. 1) of 0.08 ppm to a lower magnetic field was observed, that of C in the carbonyl group (+2 in Fig. 1, 167.79 ppm) did not change with the CIM content.

3.3. Chemical stability of binary system

Fig. 9 shows the DSC and TG-DTA/MS curves for the CIM-INDO systems. In the TG curve of the CIM-INDO system, weight loss during heating was observed at about 70°C with small endothermic peaks in the DSC and DTA curves. In order to determine the cause of the weight loss during heating, TG-DTA/MS measurements were performed. A change in the intensity of fragment peaks with heating was found for only two peaks, $m/e = 18$ and $m/e = 44$, and they were plotted against temperature. The peaks $m/e = 18$ and $m/e = 44$ were considered to be water and carbon dioxide molecules, respectively. TG-DTA/MS measurements indicated that the broad endothermic peaks with weight loss at about 70 and 150°C were attributable to the release of adsorbed water and decarboxylation of INDO, respectively. This weight loss was not observed in the case

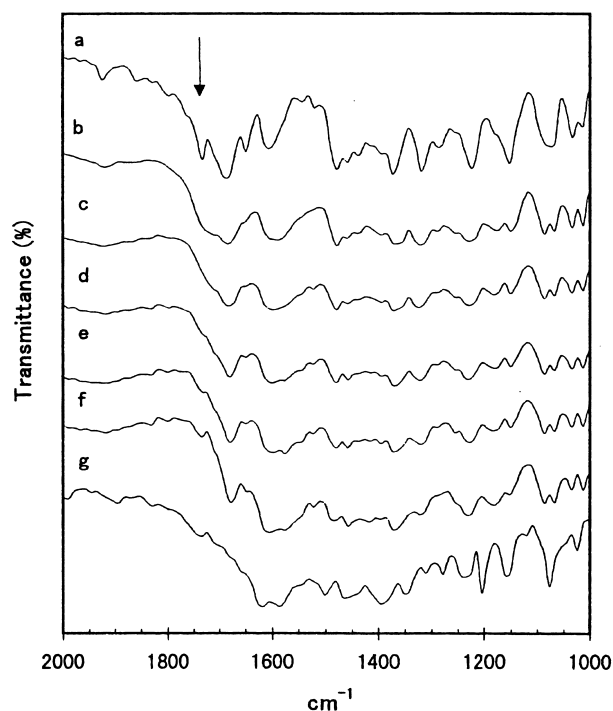


Fig. 6. FTIR spectra for CIM-INDO precipitates prepared with various compositions: (a), CIM-INDO (0:100); (b), CIM-INDO (20:80); (c), CIM-INDO (40:60); (d), CIM-INDO (50:50); (e), CIM-INDO (60:40); (f), CIM-INDO (80:20); (g), CIM-INDO (100:0).

of physical mixture of CIM-INDO, indicating that no decarboxylation occurred at temperature up to 180°C.

3.4. Phase solubility diagrams

Fig. 10 shows the phase solubility diagrams for PHEN, SA and INDO at various concentrations of in CIM solutions. Although the solubility of PHEN and SA did not change as the CIM concentration was increased, that of INDO increased linearly with increasing CIM content. These results indicate that the interaction between CIM and INDO may increase the solubility of INDO.

4. Discussion

X-ray diffraction and thermal analysis findings suggest that the CIM-INDO system becomes amorphous only upon precipitation from ethanol solution. On the other hand, amorphous precipitates were not formed in the case of the CIM-PHEN and CIM-SA systems of any composition. As reported before, the CIM and naproxen (NAP) system was found to become amorphous upon precipitation from ethanol solution [21]. Although there are many reports in the literature about preparation of amorphous systems by precipitation of drugs with polymers [17–19], little research

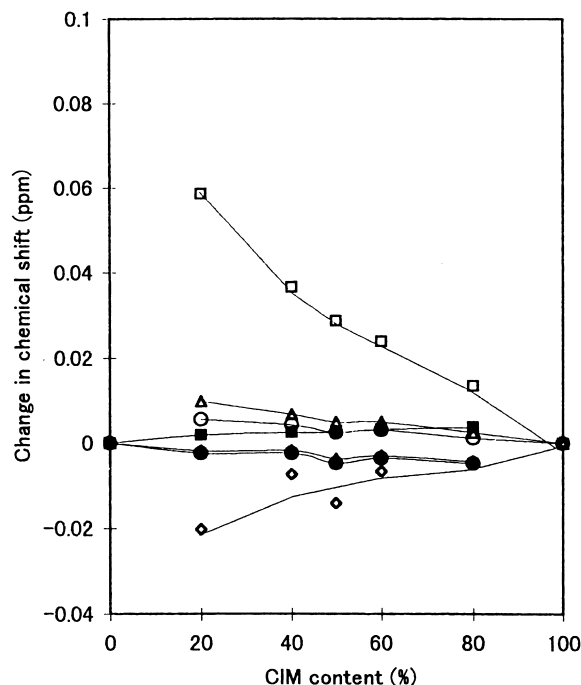


Fig. 7. Changes in ^1H -NMR chemical shift of some protons of CIM and INDO in CIM-INDO systems. (Δ) CH_3 - bound with the imidazole ring of CIM (*1, 2.13 ppm); (\square) H bound with C in the imidazole ring of CIM (*2, 7.45 ppm); (\circ), $-\text{CH}_2-$ in SCH_2 of CIM (*3, 2.58 ppm); (\diamond), H in $-\text{NHCH}_3$ of CIM (*4, 7.24 ppm); (\bullet), CH_3 - bound with the indole ring of INDO (*5, 2.22 ppm); (\blacktriangle), H bound with indole of INDO (*6, 7.04 ppm); (\blacksquare), H bound with the benzene ring of INDO (*7, 7.63 ppm). Symbols *1–*7 correspond to protons expressed in Fig. 1. The chemical shifts in parentheses are the values obtained for intact drugs.

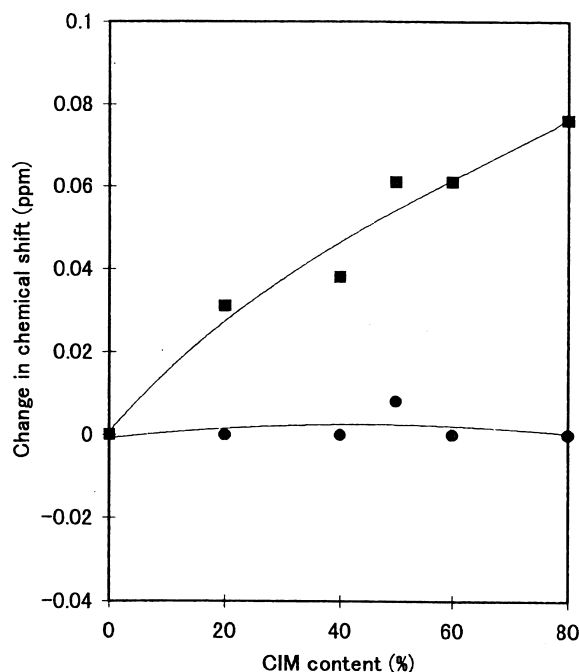


Fig. 8. Changes in ^{13}C -NMR chemical shift of some carbons of INDO in CIM-INDO systems (\blacksquare), C in COOH of INDO (+1, 171.89 ppm); (\bullet), C in CO in INDO (+2, 167.79 ppm). Symbols of +1 and +2 correspond to carbons expressed in Fig. 1.

has been published about amorphous systems prepared using low molecular weight compounds without melting. CIM is considered to be used for the preparation of amorphous systems in the case of particular molecules, such as

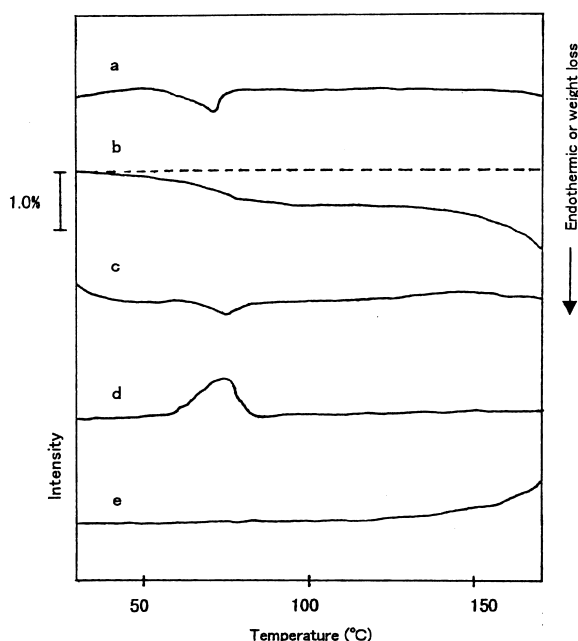


Fig. 9. DSC and TG-DTA/MS curves for CIM-INDO precipitate. (a) DSC curve; (b), TG curve; (c), DTA curve; (d), fragment peak at $m/e = 18$; and (h), fragment peak at $m/e = 44$.

NAP and INDO, only upon precipitation without heating. We have also reported the interaction between a hydrogen in the imidazole ring of CIM and carboxyl group of NAP as indicated by the results of ^1H -NMR and FTIR spectroscopy [22]. In the CIM-INDO system, a marked change in chemical shift was found only for a hydrogen of the imidazole ring of CIM and the C in COOH of INDO by ^1H -NMR and ^{13}C -NMR measurements (Figs. 7 and 8) the same as the CIM-NAP system. These results suggest the presence of an intermolecular interaction between a hydrogen of the imidazole ring of CIM and the carboxyl group of other drugs. The existence of an interaction between CIM and INDO is also supported by the modification of the peak of $\nu_{\text{C=O}}$ in carboxyl group of INDO observed in the FTIR spectra (Fig. 6). The interaction between CIM and INDO molecules would prevent the three-dimensional arrangement of both molecules; consequently the precipitate would be amorphous. Because there was little change in chemical shift observed in the case of the C of carbonyl in COCH_3 of PHEN, the C in CONH_2 of SA and the C in CO of INDO, it is evident that there is no strong interaction between CIM molecules and the carbonyl group.

Although individual CIM and INDO powders did not show weight loss at temperatures up to the melting point, the CIM-INDO system showed weight loss below the melting temperature (Fig. 9). Weight loss at about 70 and 150°C can be attributed to the release of adsorbed water and decarboxylation of INDO, corresponding to the change in intensity of the fragment peaks $m/e = 18$ and $m/e = 44$, respectively. These results indicate that the chemical stability of the CIM-INDO system decreased upon precipitation

of the binary system. Interaction between CIM and INDO may be responsible for the decrease in the chemical stability of the CIM-INDO system. The result would be that molecules in an amorphous system would be more unstable than those in a crystal.

While the solubility of INDO was found to increase with CIM concentration, no such increase in solubility of PHEN and SA was observed (Fig. 10). The increase in solubility of INDO may be due to its interaction with CIM in ethanol solution. The stoichiometry of complexation would not be 1:1, because 0.01 M CIM was effective to increase the solubility of INDO at a concentration greater than 0.01 M. This result suggests that each CIM molecule may interact with more than one INDO molecule and thereby increase the solubility of INDO. Increase of solubility would result in an increase of dissolution rate, so the binary system of CIM-INDO would have better a absorption characteristic with the prevention of the side-effect of gastrointestinal disorders of INDO.

5. Conclusion

We have shown that INDO powder became amorphous only upon precipitation with CIM in ethanol solution, when the CIM content was in the range of 20–80%. In this binary system, an intermolecular interaction between CIM and INDO was demonstrated by means of FTIR and NMR. The interaction appears to be the result of hydrogen bonding between a hydrogen in the imidazole ring of CIM and carboxyl group of INDO. This interaction would prevent

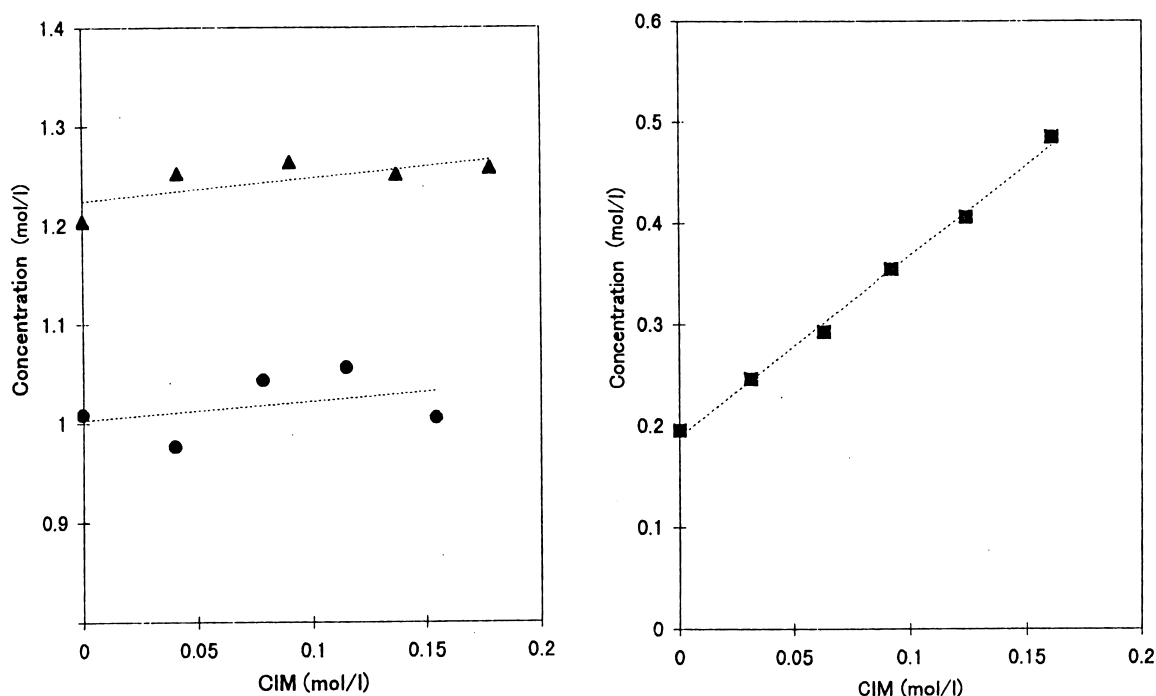


Fig. 10. Phase solubility diagrams for CIM-PHEN, CIM-SA and CIM-INDO systems. (●) CIM-PHEN; (▲), CIM-SA; (■), CIM-INDO.

the three-dimensional arrangement of individual molecules, and as a result the precipitate would be amorphous. The physicochemical stability of the CIM-INDO system decreased upon precipitation and the solubility of INDO increased in the presence of CIM. The interaction between CIM and molecules with a carboxyl group can be applied to the preparation of amorphous systems only upon precipitation without heating.

References

- [1] W.L. Chiou, S. Niazi, Phase diagram and dissolution-rate studies on sulfathiazol-urea solid dispersion, *J. Pharm. Sci.* 60 (1971) 1333–1338.
- [2] W.L. Chiou, Pharmaceutical applications of solid dispersion systems: X-ray diffraction and aqueous solubility studies on griseofulvin–polyethylene glycol 6000 systems, *J. Pharm. Sci.* 66 (1997) 989–991.
- [3] G.K. Vudathala, J.A. Rogers, Dissolution of fludrocortisone from phospholipid coprecipitates, *J. Pharm. Sci.* 81 (1992) 282–286.
- [4] W.L. Chiou, S. Riegelman, Oral absorption of griseofulvin in dogs: increased absorption via solid dispersion in polyethylene glycol 6000, *J. Pharm. Sci.* 59 (1970) 937–942.
- [5] H. Sekikawa, M. Nakano, T. Arai, Inhibitory effect of polyvinylpyrrolidone on the crystallization of drugs, *Chem. Pharm. Bull.* 26 (1978) 118–126.
- [6] M.P. Oth, A.J. Moes, Enhanced in-vitro release of indomethacin from non-aqueous suspensions using indomethacin–polyvinylpyrrolidone coprecipitate, *Int. J. Pharm.* 24 (1985) 275–286.
- [7] J.E. Hilton, M.P. Summers, The effect of polyvinylpyrrolidones on intestinal ulceration caused by indomethacin, *Int. J. Pharm.* 32 (1986) 13–20.
- [8] N. Kondo, T. Iwao, K. Hirai, M. Fukuda, K. Yamanouchi, M. Miyaji, Y. Ishihara, K. Kon, Y. Ogawa, T. Mayumi, Improved oral absorption of enteric coprecipitates of poorly soluble drug, *J. Pharm. Sci.* 83 (1994) 566–570.
- [9] S.L. Shamblin, L.S. Taylor, G. Zografi, Mixing behavior of colyophilized binary systems, *J. Pharm. Sci.* 87 (1998) 694–701.
- [10] M. Morita, S. Hirota, Effect of crystallinity on the percutaneous absorption of corticosteroid II. Chemical activity and biological activity, *Chem. Pharm. Bull.* 33 (1985) 2091–2097.
- [11] K. Yamamoto, M. Nakano, T. Arita, Y. Nakai, Dissolution behavior and bioavailability of phenytoin from a ground mixture with microcrystalline cellulose, *J. Pharm. Sci.* 65 (1976) 1484–1488.
- [12] A.P. Simonelli, S.C. Mehta, W.I. Higuchi, Dissolution rates of high energy sulfathiazole–povidone coprecipitates II: characterization of form of drug controlling its dissolution rate via solubility studies, *J. Pharm. Sci.* 65 (1976) 355–361.
- [13] K. Takayama, N. Nambu, T. Nagai, Factors affecting the dissolution of ketoprofen from solid dispersions in various water-soluble polymers, *Chem. Pharm. Bull.* 30 (1982) 3013–3016.
- [14] E. Fukuoka, M. Makita, S. Yamamura, Some physicochemical properties of glassy indomethacin, *Chem. Pharm. Bull.* 34 (1986) 4314–4321.
- [15] M.J. Pikal, A.L. Lukes, J.E. Lang, Thermal decomposition of amorphous β -lactam antibacterials, *J. Pharm. Sci.* 66 (1977) 1312–1316.
- [16] M.A. Moustafa, A.R. Ebani, S.A. Khalil, M.M. Motawi, Sulphamethoxydiazine crystal forms, *J. Pharm. Pharmacol.* 23 (1971) 868–874.
- [17] H. Sekikawa, M. Nakano, T. Arita, Dissolution mechanisms of drug–polyvinylpyrrolidone coprecipitates in aqueous solution, *Chem. Pharm. Bull.* 27 (1979) 1223–1230.
- [18] Q. Lu, G. Zografi, Phase behavior of binary and ternary amorphous mixtures containing indomethacin, citric acid and PVP, *Pharm. Res.* 15 (1998) 1202–1206.
- [19] G. Van den Mooter, N. Augustijns, R. Blaton, Physico-chemical characterization of solid dispersions of temazepam with polyethylene glycol 6000 and PVP K30, *Int. J. Pharm.* 164 (1998) 67–80.
- [20] M.P. Summers, R.P. Enever, Preparation and properties of solid dispersion system containing citric acid and primidone, *J. Pharm. Sci.* 65 (1976) 1613–1617.
- [21] R.J. Timko, N.G. Lordi, Thermal characteristics of citric acid solid dispersion with benzoic acid and Phenobarbital, *J. Pharm. Sci.* 68 (1979) 601–605.
- [22] S. Yamamura, M. Momose, K. Takahashi, S. Nagatani, Solid-state interaction between cimetidine and naproxen, *Drug Stability* 50 (1996) 173–178.
- [23] L.S. Taylor, G. Zografi, Spectroscopic characterization of interactions between PVP and indomethacin in amorphous molecular dispersions, *Pharm. Res.* 14 (1997) 1691–1698.